51st AIAA Aerospace Sciences Meeting including the New Horizons Forum and Aerospace Exposition
07 - 10 January 2013, Grapevine (Dallas/Ft. Worth Region), Texas

AIAA 2013-0871

Going for Experimental and Numerical Unsteady Wake Analyses Combined with Wall Interference Assessment by Using the NASA CRM Model in ETW

Thorsten Lutz[*] and Philipp P. Gansel[†]
University of Stuttgart, 70569 Stuttgart, Germany

Jean-Luc Godard[‡]
ONERA, The French Aerospace Lab, F-92190 Meudon, France

Anton Gorbushin[§]
Central Aerohydrodynamic Institute, Zhukovsky, Moscow reg., 140180, Russia

Robert Konrath[¶]
German Aerospace Center (DLR), Institute of Aerodynamics and Flow Technology, 37073 Göttingen, Germany

Jürgen Quest[#]
European Transonic Windtunnel GmbH, 51147 Cologne, German

and

S. Melissa B. Rivers[**]
NASA Langley Research Center, Hampton, VA 23681

Detailed experimental and accompanying numerical studies on the development of unsteady wakes past an aircraft under stall conditions are currently prepared by a consortium of research institutions and universities. The experiments will be performed in the ETW cryogenic wind tunnel on the NASA Common Research Model. Besides wake surveys using time-resolved cryo PIV measuring technique, wall interference measurements are planned. The tests scheduled for July 2013 are funded by the European Commission in the 7th framework program. In this paper results of preparatory CFD studies and wake analyses of the CRM model, the TR-PIV measuring technique and the ETW facility are presented along with the wind tunnel model and the planned test program.

Nomenclature

CFD	=	Computational Fluid Dynamics
CRM	=	Comon Research Model
b	=	wing span
c	=	reference chord
c_l	=	lift coefficient
c_p	=	pressure coefficient
DES	=	Detached Eddy Simulation

[*] Senior Researcher, Institute of Aerodynamics and Gas Dynamics, Pfaffenwaldring 21, Senior member AIAA.
[†] Research Engineer, Institute of Aerodynamics and Gas Dynamics, Pfaffenwaldring 21.
[‡] Research Engineer, Applied Aerodynamics Department.
[§] Head of Laboratory, Aerodynamic Department.
[¶] Research Scientist, Institute of Aerodynamics and Flow Technology.
[#] Chief Aerodynamicist & External Project Manager, AIAA Associated Fellow.
[**] Research Engineer, Configuration Aerodynamics Branch, Mail Stop 267, Senior Member AIAA.

DPW = Drag Prediction Workshop
ESP = Electronically Scanned Pressure
$ESWI^{RP}$ = European Strategic Wind Tunnels Improved Research Potential
ETW = European Transonic Windtunnel
f = frequency
HTP = horizontal tail plane
k = turbulence kinetic energy
L = turbulence length scale
L_{11} = longitudinal integral length scale
LES = Large Eddy Simulation
LU-SGS = lower-upper symmetric Gauss-Seidel
M_∞ = freestream Mach number
NTF = National Transonic Facility
(U)RANS= (unsteady) Reynolds-Averaged Navier-Stokes
Re = Reynolds number based on the reference chord length
RMS = Root Mean Square
S = wing reference area
St = Strouhal number
T_t = total temperature
TR-PIV = Time-Resolved Particle Image Velocimetry
U = velocity
U_∞ = freestream velocity
x,y,z = Cartesian coordinates
y^+ = wall distance normalized by the viscous length scale

α = angle of attack
ε = dissipation rate of turbulent kinetic energy
η = spanwise position normalized by the wing half span

I. Introduction

The knowledge and the understanding of aerodynamic phenomena around aircraft for conditions at the limit of the flight envelope is still to be improved and the prediction of such phenomena remains a challenge. This statement applies in particular to the aerodynamic stall. The aircraft stall is characterized by massive flow separation on the wing. Such phenomenon is highly unsteady and presents large scale turbulent fluctuations. As a consequence, the wake downstream of the wing shows the same behavior. The unsteady wake can affect the flow about the empennage, impact the efficiency of the control surfaces and excite structural responses. This holds for both, low speed and high speed stall. These effects are safety critical and the characterization of the unsteady empennage inflow conditions as well as the improved understanding and prediction of these interaction effects is therefore of high interest for the aircraft industry. This includes studies on the development of the velocity spectrum downstream of the wing trailing-edge along with the driving physical mechanisms.

In the transonic buffet regime, complex interaction between an oscillating three-dimensional shock front and the pulsating separation area occurs. This interaction is associated with unsteady surface pressures on the wing with the fluctuations being propagated to the wake. While for 2D airfoils the surface and wake spectra are characterized by particular frequencies, a broadband frequency spectrum can be observed for three-dimensional wings[21]. The 3D buffet phenomenon and its impact on the development of the unsteady wake towards the empennage is currently far from being understood and only very few investigations have been published[14, 15, 21, 29]. Low speed stall is driven by pressure induced flow separation from the wing at high angle of attack. The separated wake shows strong unsteadiness, a broadband frequency spectrum and large scale turbulent structures. There are many numerical and experimental investigations on flow separation from wings and airfoils and its impact on the aerodynamic characteristics [6, 7, 8, 11, 17, 23, 32, 33, 34]. But apart from research on tip vortex roll-up there are only few studies on the development of the separated wake spectrum downstream of the trailing edge. Experimental investigations on the development of the unsteady wake flow field are limited to measurements on airfoils at low Reynolds number[27] or studies on the impact of flow control devices at low Re[18].

A literature survey reveals that there is a lack in numerical and experimental wake studies for 3D configurations and the impact on the empennage aerodynamics although appropriate numerical and experimental methods are available nowadays. In particular time-resolved wake measurements for realistic aircraft configurations at flight

Reynolds and Mach numbers are missing. Such experiments are highly desired for flow physics studies and to validate numerical methods, like URANS with advanced turbulence models or hybrid RANS-LES approaches. The ESWI[RP] sub-project "Time-resolved wake measurements of separated wing flow and wall interference measurements" has been launched with the objective of answering to this need. ESWI[RP] ("European Strategic Wind Tunnels Improved Research Potential") is an integrating research activity funded by the European Commission in the 7th framework programme. The objective is to enable trans-national access to dedicated testing facilities, to stimulate networking activities and to increase the capacity of the participating wind tunnels by demonstration of advanced measuring techniques and new hardware (see ESWI[RP] website: www.eswirp.eu). Three sub-projects were accepted, one for tests in each of the involved facilities which are the large subsonic DNW-LFF wind tunnel, the transonic ONERA S1MA tunnel and the pressurized cryogenic ETW facility.

The present sub-project comprises measurements in the ETW (European Transonic Windtunnel) which enables experiments on full aircraft configurations at flight Reynolds and Mach number. Detailed flow-field wake surveys by time-resolved particle image velocimetry (TR-PIV) measurements of an aircraft configuration at low and high speed stall conditions will be performed. Latest cryo PIV technique[16] will be employed by DLR to ensure highly resolved flow field data. One important objective of the project is to create an experimental data base available to the whole research community for flow physics studies and code validation purposes. This requires to consider a generic but realistic aircraft configuration with public available geometry. The wind tunnel model of the NASA Common Research Model (CRM) represents an ideal configuration[30] fulfilling these requirements. The CRM model will be provided by NASA for the planned ETW tests scheduled for July 2013.

Supplementary to the wake measurements, studies on wall interference effects are planned in this ESWI[RP] sub-project. Wind tunnel wall interference is still an important issue for increasing the accuracy of test results during the aircraft design phase. In recent years, the manufacturers of transport aircraft have been imposing more and more stringent requirements for the accuracy of experimental investigations in wind tunnels. This is caused by the needs on a more reliable determination of aerodynamic characteristics of the aircraft and, accordingly, its economic effectiveness. Striving for most accurate performance measurements in wind tunnels requires enhanced knowledge on interference effects introduced by the flow boundaries. Considering slotted wall wind tunnels, the subject appears extremely complex due to the presence of strongly 3-dimensional slot flow and the non-homogenous boundary condition. Several groups of investigators worked on slotted wall interference. A list of references on this problem is given in Refs [1, 24].

Currently the possibility appears to apply CFD methods for the problem of permeable wall interference due to significant increase of computer operation memory and calculation speed[3, 5, 20]. A special software Electronic Wind Tunnel (EWT) was developed at TsAGI to support wind tunnel testing[4]. ONERA applied CFD methods to develop wall interference methodology[13, 31]. New CFD approach for wall interference investigations requires additional experimental data (for example wing deformation) in comparison with classical methods. Therefore the necessity appeared to perform wall interference experiments in the ETW at the new level of technology. The main objectives of the planned wall interference investigations is to increase the accuracy and reliability of ETW wall interference corrections, to investigate the Reynolds number influence on wall interference and to form a test case for the verification and validation of CFD tools for in-tunnel simulations.

In addition to the experiments, numerical activities will be conducted before the tests to support the definition of the test programme and after the tests for a numerical / experimental validation. CFD computations using unsteady RANS and hybrid RANS / LES methods for low speed as well as for high speed conditions. The validation will be based on aerodynamic forces and pressure distributions on the configuration and on flow characteristics measured or calculated in the field.

The ESWI[RP] sub-proposal was submitted by a consortium of renowned European research institutions and universities. Besides ONERA (Aerospace research center) from France as project leader, University of Stuttgart and DLR (German Aerospace Center) from Germany, TsAGI (Central Aerohydrodynamic Institute) from Russia, ICAS (Institute of Thermomechanics) and VZLU (Aerospace research and test establishment) from Czech Republic, VKI (von Karman Institute for Fluid Dynamics) from Belgium and UCAM (University of Cambridge) are members of the team. Currently the TR-PIV measuring system is adapted and tested to ensure highly resolved measurements under cryogenic conditions in the wake region of interest. At the same time preparatory numerical studies are performed to define appropriate test conditions and to identify relevant locations for the wake measurements.

The present paper describes the current status of the preparation and is organized as follows. Sec. 2 gives an overview about the ETW facility and the CRM wind tunnel model. In Sec. 3 CFD studies by University of Stuttgart on the CRM model are discussed while Section 4 gives some details of the planned wake and wall interference measurements and describes the cryo TR-PIV measuring technique to be used.

II. Wind Tunnel and Common Research Model

A. Description of the CRM wind tunnel model

The model to be used in this investigation is the NASA Common Research Model (CRM)[30,] which was initially designed to be the basis for the fourth AIAA drag prediction workshop (DPW-IV)[32]. This configuration consists of a contemporary supercritical transonic wing and a fuselage that is representative of a wide-body commercial transport aircraft. The CRM is designed for a cruise Mach number of $M_\infty = 0.85$ and a corresponding design lift coefficient of $c_l = 0.5$. The aspect ratio is 9.0, the leading edge sweep angle is 35°, the wing reference area S is 3.01 ft^2 (0.280 m^2), the wing span b is 62.46 inches (1.586 m), and the mean aerodynamic chord c is 7.45 inches (0.189 m). The model moment reference center is located 35.8 inches (0.909 m) back from the fuselage nose and 2.04 inches (0.0518 m) below the fuselage centerline. Simple flow through engine nacelles can be mounted on the model; however, they will not be used in this project to provide a clean wing geometry. The CRM is instrumented for force and moment measurements, wing pressures, wing-root strain gages and dynamic pressures. The wing pressure distributions are measured on both the left and right wings using 291 pressure orifices located in 9 span-wise wing stations (η = 0.131, 0.201, 0.283, 0.397, 0.502, 0.603, 0.727, 0.846, and 0.950). The wing-root strain is measured using half bridges on both wings and the dynamic pressures are measured using Kulite sensors, which are located at approximately 70% of span of the left hand wing. The model is mounted in the wind tunnel using a blade sting arrangement as seen in Fig. 1.

Figure 1. Photo of the CRM in the Ames 11-ft Wind Tunnel

B. The European Transonic Windtunnel (ETW)

The ETW facility is a continuously operated pressurized cryogenic wind tunnel (Göttingen type) featuring slotted or solid walls. The Mach number ranges from 0.15 to 1.35 while the Reynolds number can be established by combinations of pressure (115 to 450 kPa) and temperature (110 to 313 K), hence, allowing pure Reynolds number or pure aeroelastic investigations. The test section dimensions are 2.4m x 2m x 9m (width x height x length). The length of the aerodynamic circuit is 142m. The facility can only be operated in nitrogen mode requiring a liquid nitrogen injection by spraying nozzles and venting using blow-off valves as schematically shown in Fig. 2.

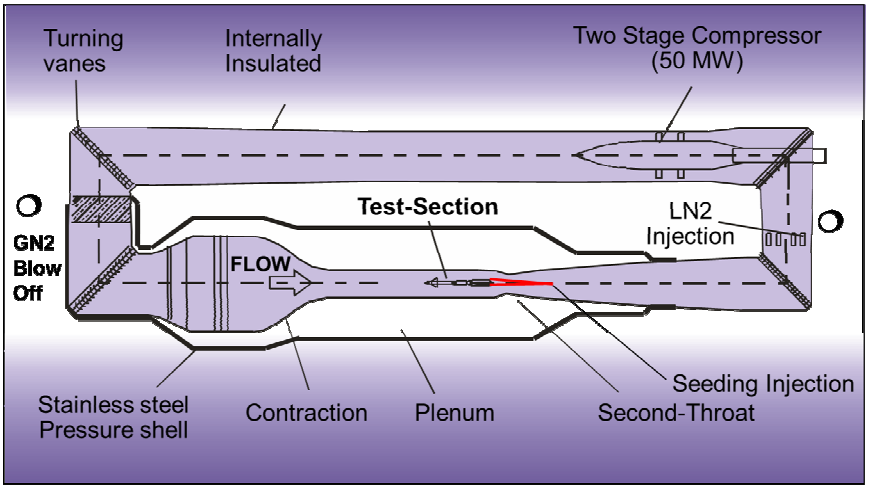

Figure 2. The aerodynamic circuit of ETW.

As the nitrogen environment prevents classical access to the circuit, models may be moved to a variable temperature room applying a model-cart transport concept. Here, the model cart consists of the model itself including its supporting system and the ceiling of the test-section linked by a voluminous structure to a sealing flange to be attached to the top of the tunnel shell. A rail based transporter allows lifting and lowering of the cart in different areas where warm-ups or cool-downs may be applied as well as the transport from or back to the test-section.

While along the major part of the circuit the tunnel shell is directly internally insulated, the settling chamber, the slotted test section and the 2nd throat area are surrounded by a 10m diameter plenum minimising wall interference. During tunnel operation pressure, temperature and density in the plenum are close to the static gas conditions of the test section main flow. This generates a drawback for all instrumentation being placed there to either withstand the operational pressure and temperature conditions or to be housed in suitable mostly thermally controlled boxes. Optical access may then be provided by using the circular windows in the test section walls as to be seen in Fig. 3.

Figure 3: Test section configurations of ETW: solid (left), slotted side-walls (centre) or slotted top/bottom walls (right).

Although ETW had originally been designed for transonic and slight supersonic speed conditions it also revealed an extraordinary high quality for low speed, high lift investigations after introducing this test capability by the beginning of this century. Dominated by the model cart concept, half models have to be attached to the test section ceiling to keep the benefit of transportability. While for half model testing the top wall represents a plane of symmetry always aligned parallel to the centreline and solid, the side-walls may be set either solid or slotted according to client's request (see Fig. 3). The availability of positions for light sheet generators as well as the voluminous TR-PIV cameras is limited by the number of windows in the test-section walls and the space envelope behind. Specific heated enclosures have to be build for housing the cameras and optical modules. Placing a module inside the floor structure requires a multiple deflection of the laser beam, entering through the tunnel side wall, by mirrors. Another

issue on the way to a functional cryo PIV was seen in the generation of tracer particles suitable for cryogenic flow. Recent tests in ETW applying standard PIV could qualify injected tiny ice crystals as an favourable material for tunnel operating conditions below the dew point.

III. Preparatory Numerical Studies

CFD simulations solving the unsteady Reynolds-Averaged Navier-Stokes (URANS) equations have been performed at the University of Stuttgart to identify relevant stall free stream conditions and the positions of interest in the wake. The simulations furthermore served to derive the required temporal and spatial resolution of the PIV measurements. The considered freestream conditions correspond to the priority 1 wind tunnel test cases (compare Sec. IV.D) in low-speed ($M_\infty = 0.25$; $Re = 17.2 \cdot 10^6$) and high-speed ($M_\infty = 0.85$; $Re = 30 \cdot 10^6$) conditions respectively. Further numerical investigations are planned to validate new numerical schemes and turbulence models using the obtained unsteady wind tunnel test results.

A. Numerical Setup

The TAU flow solver developed by DLR was used for the present studies (versions 2011.2.0 and 2012.1.0)[26]. TAU is an unstructured finite volume solver which offers a second order accurate central discretization scheme on cell-vertex median-dual grids. Scalar and matrix dissipation schemes are implemented for stabilization. For time integration backward Euler differences are employed in the used implicit LU-SGS scheme. Dual time-stepping is utilized for unsteady simulations. In the present low-speed case simulation the physical time step was set to 0.90 ms which is one hundredth of the convective time scale c/U_∞. In the high-speed buffet flow regime 150 physical time steps of 0.18 ms covered one convective time scale. The shock oscillation on the wing was discretized by approximately 2220 time steps per period. The number of inner iterations was adjusted to achieve convergence of the integral forces in each time step. For convergence acceleration local time-stepping and multi-grid cycles were applied. The one-equation model of Spalart and Allmaras[28] was used for turbulence modeling.

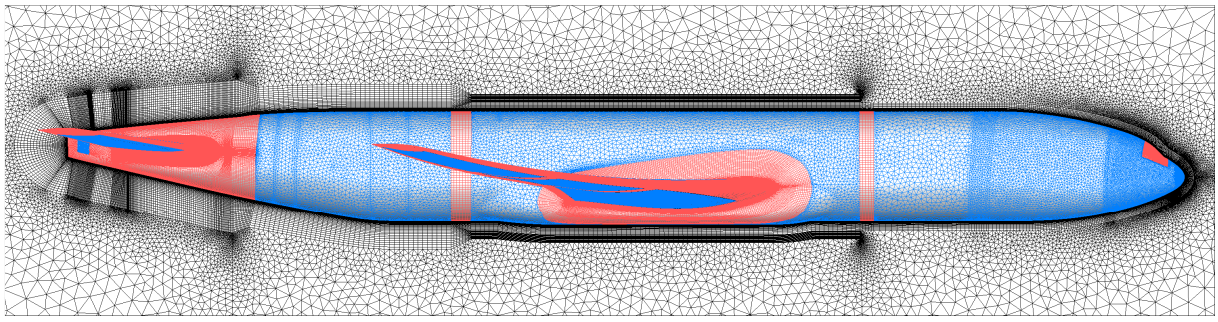

Figure 4. Side view of the low-speed stall surface grid; structured parts in red, unstructured in blue.

Using the grid generating software Gridgen V15 two different hybrid meshes were constructed, one dedicated to the low-speed test case while the other grid was adapted to the high-speed case. The boundary layer domain was discretized by a structured mesh. In order to ensure a correct boundary layer representation the grid parameters (first cell height, overall boundary layer mesh height, growing factor and number of layers) were varied in several steps along the fuselage. The different prismatic grid patches are connected with structured hexahedral blocks as shown in Fig. 4. The same procedure is applied to the wing which is divided in several spanwise segments. To facilitate a good resolution of the boundary layer in the wing-fuselage (see Fig. 5) and HTP-fuselage junctions structured hexahedral blocks were introduced in the corners in an O-type topology (compare Ref. [10]). At the leading and trailing edges structured grid block were inserted as well to take advantage of the independently adjustable resolution in streamwise and

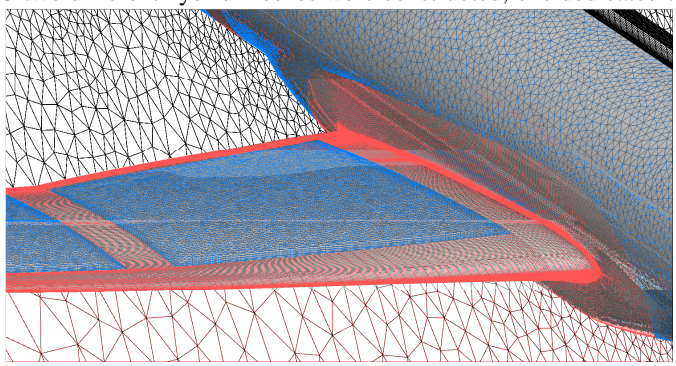

Figure 5. Detailed view on the inboard wing area of the low-speed stall grid showing the structured meshed regions.

spanwise direction. The tail cone of the fuselage is meshed entirely bock-structured. The first point distance to all surfaces is maintained to be $y_1^+ \leq 1$. The mesh for the buffet studies has an additional refinement of cells on and above the wing upper surface in the shock region. The half-spherical farfield boundary condition is placed in a distance of 25 times the fuselage length. The two meshes show a number of 19 and 21 millions grid cells, respectively.

Firstly steady RANS polar simulations were performed to identify the angle of attack where a massive separation occurs on the inboard wing upper surface. Since for the CRM wing flow separation starts on the outboard sections in the numerical studies (see Fig. 6), the considered α of 19° is far above the stall angle. This should guarantee an entirely separated flow on the inner wing sections upstream of the HTP. For $\alpha = 4.5°$ the simulations of the transonic case show buffet at the main wing. This angle of attack is also known from previous experiments to lie in the buffet range[2]. The unsteady simulations were started from a steady solution at the desired α. Beforehand the angle of attack has been increased in small steps beginning in the linear part of the lift polar. First the unsteady simulation was started with a coarse time step to launch flow unsteadiness and remove big disturbances quickly from the computational domain. Then the simulation was run with the small time step until transient effects have faded and the mean integral forces were convergent. After activation of temporal averaging of the flow field 4000 further time steps are run. During this phase the velocities and pressure coefficients at single points in the field are logged in every time step for spectral investigation. Instantaneous values, means and variances of the variables are stored for the whole flow field.

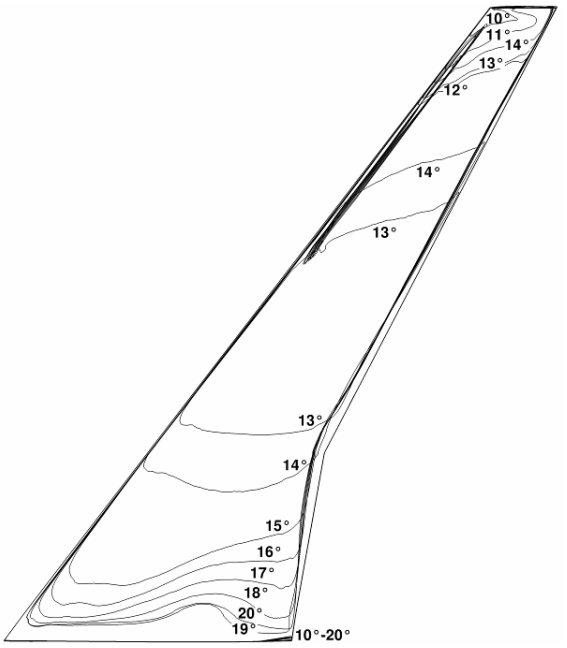

Figure 6. Regions of negative wall shear stress coefficient in *x*-direction for different angles of attack under low-speed conditions $M_\infty = 0.25$; $Re = 17.2 \cdot 10^6$ (steady calculations).

B. Evaluation of the Wake Development

An evaluation of the URANS simulations served to identify appropriate positions of the PIV planes in the wing wake. Figure 7 shows the root mean square (RMS) values of the surface pressure fluctuations in the subsonic stall flow regime. Note that the HTP and the rear part of the fuselage behind the wing are affected by the unsteady separated wing flow. Besides the wing the highest fluctuation amplitudes occur at the leading edge of the HTP.

To get an impression of the fluctuation levels in the wake, the RMS value of the c_p fluctuations was evaluated along straight lines connecting the wing trailing edge and the HTP leading edge at constant spanwise locations (as sketched in Fig. 7). The RMS values along these lines are plotted in Fig. 8 a) and b) for the low-speed and high-speed conditions, respectively. In both cases the fluctuations decrease downstream, as expected. The decay of the fluctuations covers approximately one order of magnitude for both conditions and all spanwise positions. Just upstream of the HTP leading edge the fluctuations are amplified again and gain almost their maximum level. At $M_\infty = 0.25$ the RMS values rises first to hit its maximum 0.1 m behind the wing trailing edge. This can be attributed to large turbulent wake structures that develop above the wing and approach the line of evaluation some distance downstream of the trailing edge. In the first part of the wake the highest amplitudes occur at the outer spanwise positions of 23% and 25% half span. Downstream of $x \approx 1.3$ m the situation starts to invert and at the beginning of the increase toward the HTP the strongest fluctuations are located at 15% and decrease outboards. Under transonic conditions the amplification begins a bit earlier. Here the highest amplitudes reside at the most inboard location and decrease further outwards over the whole streamwise range.

For spectral analysis the flow variables have been stored for every physical time step at 640 positions distributed in the flow field. Exemplarily, Fig. 9 shows the resulting spectra for one selected point at low and high-speed stall conditions, respectively. The frequencies on the abscissa are transformed to the geometric scale and flow conditions of the planned ETW tests using the Strouhal number *St* as dimensionless quantity. The low Mach number case spectrum shows a dominant frequency at 110 Hz followed by its higher harmonics. This indicates big coherent eddies being shed from the wing into the wake and is consistent with results of two-dimensional URANS simulations of

airfoils at low-speed stall[9]. Above 1 kHz the amplitudes fall rapidly and end in random noise. The high-speed case spectrum has its peak around 250 Hz at lower amplitudes than the low-speed curve. The drop of amplitudes also starts at higher frequencies (~2.5 kHz). The displayed spectra do not contain the modeled small scale part of turbulence due to the RANS approach. Thus for higher frequencies they show unrealistic small amplitudes.

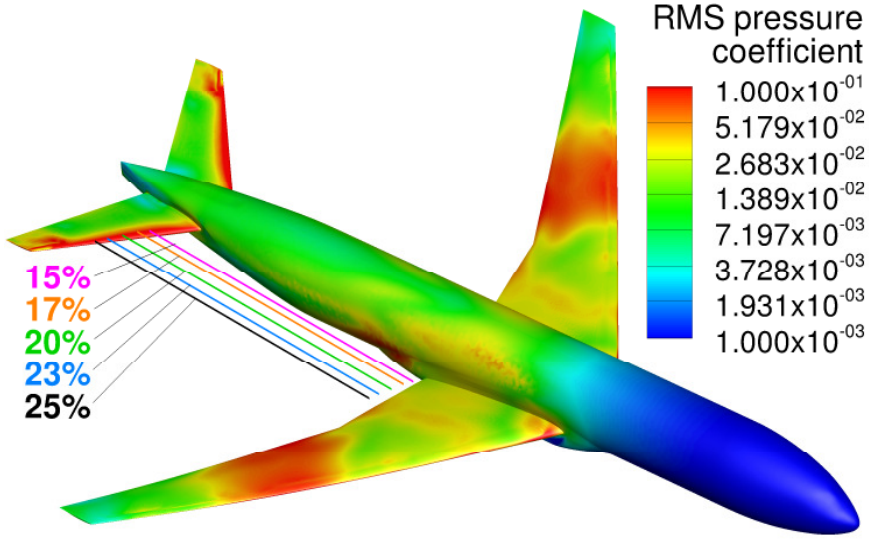

Figure 7. Evaluation positions upstream of the HTP given in percentage of half span and root mean square of surface pressure coefficient fluctuations at $M_\infty = 0.25$, $Re = 17.2 \cdot 10^6$, $\alpha = 19°$.

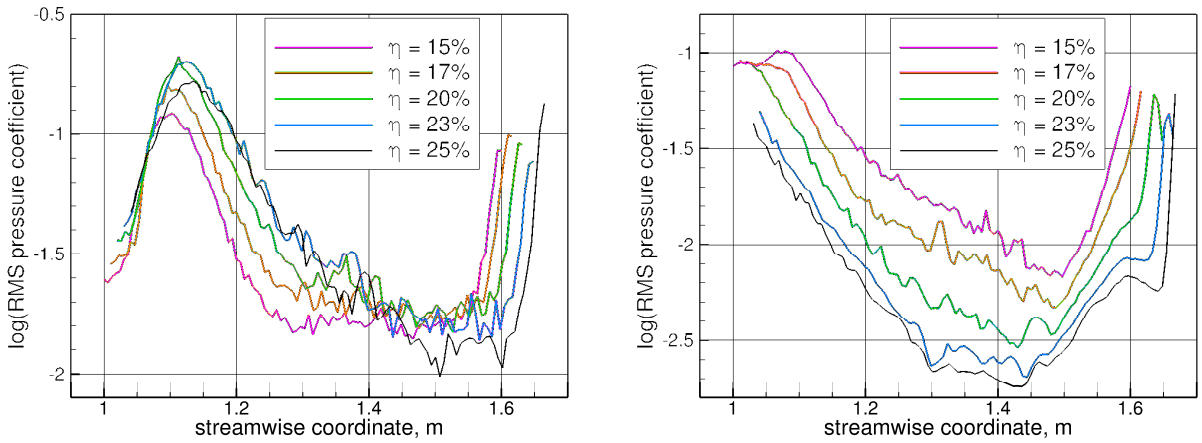

Figure 8. Root mean square of the pressure coefficient in the wing wake upstream of the HTP at a) $M_\infty = 0.25$, $Re = 17.2 \cdot 10^6$, $\alpha = 19°$ and b) $M_\infty = 0.85$, $Re = 30 \cdot 10^6$, $\alpha = 4.5°$.

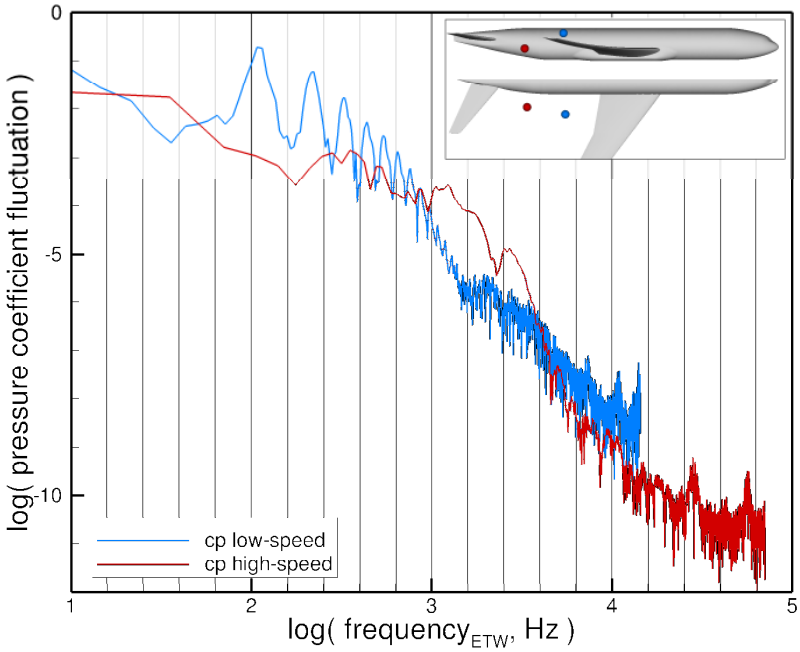

Figure 9. Spectral content of resolved pressure fluctuation and energy spectrum function based on turbulence model entities at three points in the wake flow.

IV. Planned Wake and Wall Interference Measurements

A. Requirements for the PIV Measurements

The required temporal and spatial resolution of the TR-PIV wake measurements were estimated based on the URANS simulations described in Sec. III, URANS and DES calculations of stalled airfoils[9] and on information from literature on expected dominating frequencies. From existing unsteady high-speed buffet measurements on the CRM configuration at $Re = 5 \cdot 10^6$ the dominant frequency band of pressure fluctuations on the wing upper surface is found close to 400 Hz[2], corresponding to $St = 0.266$. In agreement with this the frequency range of the strong turbulent fluctuations on another wing-body configuration appears at Strouhal numbers from 0.206 to 0.535 for similar free flow conditions ($M_\infty = 0.82$, $Re = 2.5 \cdot 10^6$)[21]. The URANS simulations of the CRM conducted by IAG (see previous section) provide a peak Strouhal number of 0.272 which compares well with the experimental results.

The expected peak frequencies for the low-speed stall conditions are lower than that. In wind tunnel measurements of a transport aircraft in stall a dominant frequency of $St \approx 0.027$ was measured[12]. From URANS simulations of the airfoil stall test case from Ref.[27] a vortex shedding Strouhal number from the trailing edge of 0.076 was determined. Scaled to the low-speed stall conditions of the CRM tests planned in the ETW these dimensionless figures result in frequencies of 8.83 Hz and 24.6 Hz. The unsteady CFD simulation of the CRM in low-speed stall, however, showed a considerably higher peak frequency of 110 Hz and $St = 0.385$ respectively. In conclusion peak frequencies in the range of around 100 to 250 Hz are expected for the intended ETW test conditions. In order to obtain adequate information about the characteristics of the wake spectra and considering the requirements of the Nyquist sampling theorem a temporal resolution of 1 kHz was deemed sufficient for the planned TR-PIV tests.

The estimation of the required spatial PIV resolution was based on the integral turbulent length scales derived from the URANS calculations. The modeled k and ε values were estimated from the velocity field and turbulent viscosity values. The integral longitudinal length scale L_{11}, when integrated from a modeled turbulence spectrum shows a constant ratio L_{11} / L with the length scale $L = k^{3/2}/\varepsilon$. For high Taylor-scale Reynolds numbers (which are in the range of 1000 in the wake area) this ratio is converging to 0.43[22]. In comparison Lysack and Brungart give a L_{11}/L-ratio of 0.39 for a similar turbulence spectrum model[19]. In Figure 10 the L_{11}-distribution is given in y-planes at 20% half span in the low-speed case (left) and at 15% half span at high-speed (right). Here the values are scaled to the dimensions of the wind tunnel model. While the largest length scales are around 20 mm in the low-speed stall case

and somewhat smaller at high-speed buffet (~17 mm), most of the wake shows length scales in the range of 10 mm. To characterize eddies of this size a resolution around 1 mm is aspired.

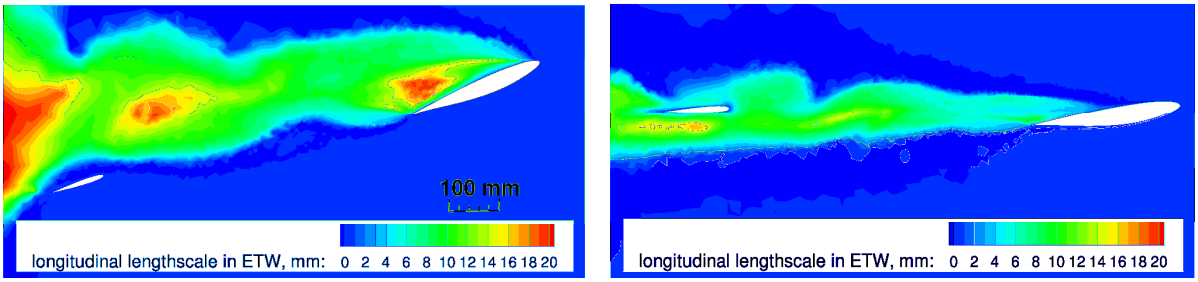

a) b)

Figure 10.Instantaneous distribution of longitudinal lengthscale L_{11} in the wake at a spanwise position of a) $\eta = 20\%$ ($M_\infty = 0.25$, $Re = 17.2 \cdot 10^6$, $\alpha = 19°$) and b) $\eta = 15\%$ ($M_\infty = 0.85$, $Re = 30 \cdot 10^6$, $\alpha = 4.5°$).

The PIV measurement planes will be oriented in y = const. planes, i.e. parallel to the symmetry plane. To obtain significant results, positions will be chosen where high fluctuation levels are expected from the preparatory CFD simulation (see Sec. B.III). Three different positions are considered in both free-stream cases, where the highest priority is assigned to the flow region directly upstream of the HTP leading edge, followed by a location shortly downstream of the wing trailing edge and a third one in the middle. By this setting it is possible to investigate the development and the propagation of the turbulence by correlating the different streamwise.

B. TR-PIV System and Experimental Set-Up in the ETW

According to the definition of the requirements (see last subsection), the wake measurements will be performed using a time-resolved PIV system which is based on components developed by DLR in cooperation with ETW for PIV applications in the pressurized cryogenic wind tunnel ETW to make flow field investigations at flight Mach and Reynolds numbers of transport aircraft possible. For a successful PIV application under the specific conditions of ETW, particular adaptations of the PIV technique were necessary with regard to:

- the generation of suitable tracer particles in the ETW
- the control of beam deflections of pulsed laser light while passing the plenum
- a placement of optical components within the cryogenic environment
- optical effects at high pressures (450 kPa) and low temperatures (110 K)

The ETW circuit is internally cladded with porous insulation material, which means that there is a risk of permanent damage of this material when using oil droplets as flow tracers that are commonly used in conventional wind tunnels. The droplets can accumulate on the floor and penetrate into the insulation material. Therefore, new seeding techniques (Fig. 11a) have been tested in the ETW using ice particles (H_2O) at cryogenic temperatures ($T_t \leq 230$ K); these evaporate completely during a warm-up. However, the formation of ice particles in the wind tunnel must be controlled carefully to produce tracers in the correct size ranging from about 0.5 µm to 2 µm; i.e. small enough to keep the difference between flow and particle velocities negligibly small and yet large enough for detectable light scattering off them using digital cameras. The formation, growth and sublimation of ice particles, however, depend on the dew point, pressure and temperature of the test gas. Also the amount of injected water must be kept small in order to preclude icing on the test section walls.

The developed cryo PIV system consists also of special optical modules (Fig. 11b) for a placement of cameras and light sheet optics behind the window openings of the test section. Because of the cryogenic environment, these modules are placed in heated housings. The PIV laser is placed outside the wind tunnel and the laser beam is directed via laser mirrors through a small window in the plenum pressure shell to an optical module (containing the light-sheet-forming optics) installed in the test section wall (compare Fig. 12). To compensate for laser light beam deflections due to optical and mechanical effects when changing the tunnel temperature or pressure, a beam monitor is employed in this module which permits automatic repositioning and redirection of the laser beam using motorized mirrors. The light sheet orientation and thickness in the measurement region of the flow can also be set remotely. For an optimization of the particle imaging under cold and pressurized conditions, the modules for the PIV cameras allow for a remote adjustment of the lens focus, Scheimpflug angle and lens F-number. Figure 11c shows the meas-

ured vortical flow at a downstream position on a transport aircraft model wing that was obtained in the ETW at T_t = 125 K[25].

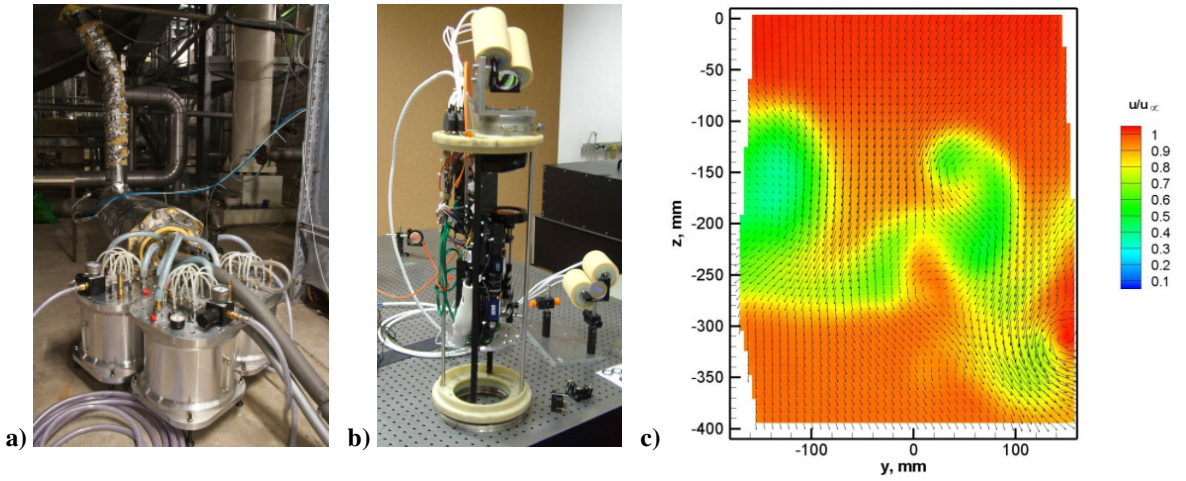

Figure 11.a) Ice particle seeding system at ETW b) preparation of light-sheet optics module of cryo PIV system in the laboratory c) PIV result of the vortical flow field downstream the wing of an aircraft model obtained at T_t = 125 K and a Reynolds number of 6 million.

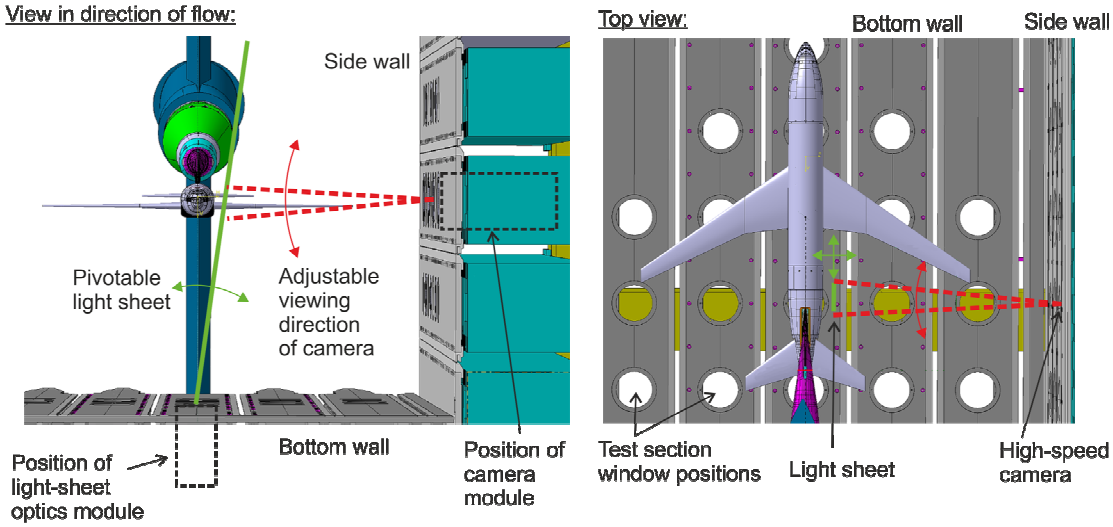

Figure 12. Planned arrangement of time-resolved PIV in the ETW for a measurement of the turbulent wake of the wing in front of the horizontal tip wing.

The optical arrangement for the planned time-resolved PIV investigations is shown in Fig. 12. To fulfill the required measurement rate of 1 kHz for the transonic case, a LEE LDP-200MQG high-speed laser will be used, emitting light energies of 2 x 20 mJ per pulse. This means that the particle images must be recorded with a frequency of 2 kHz, for which a pco.dimax high-speed CMOS camera is to be used. This camera can be precisely triggered and is capable of recording two subsequent images with a short time separation of only 3.5 µs, which is just short enough for the measurement of the expected highest velocities for the transonic case. The light sheet is aligned parallel to the direction of the free stream velocity for a good dynamic range of the measured velocities, which is important to enable a resolution of the turbulent fluctuations. To achieve high enough light densities within the light-sheet, its height is limited to about 50 mm. As shown in Fig. 12 the light-sheet box is located behind a window in the bottom wall. However, a window opening directly below the flow region of interest is not available, therefore the module is placed at the window in the middle row which is closest in position to the region of interest. Different measurement positions are achieved by pivoting the light-sheet accordingly, for which the light-sheet module is equipped with

motorized mirrors. According to the different measurement plane positions and orientations, the lens of the camera must be re-adjusted with respect to the viewing direction, focus and the Scheimpflug angle for which a specific lens adapter and a mirror setup will be designed and fabricated. In addition, a new camera housing with larger dimensions is needed for the setup, due to the size of the pco.dimax camera. The high-speed camera provides a resolution of 2016 x 2016 px for recording rates of max. 1.1 kHz. For a recording rate of 2 kHz, the resolution has to be reduced to 1920 x 1080 px. Using PIV planes of 100mm x 50mm the requirements for the spatial resolution discussed in Sec. IVa. are by far fulfilled. The high spatial resolution moreover enables to obtain information about the high frequency domain of the wake spectrum utilizing Taylor's frozen-turbulence hypothesis by evaluating the data of an instantaneous PIV velocity field along streamlines or – in the first approximation – along the main flow direction. The image data is stored first in the internal camera RAM of 36 GB, which can store 2300 or 4600 double images at full or reduced pixel resolution, respectively. Considering 1000 samples for a single time series to be sufficient for a statistical data analysis, a read-out of the camera RAM is necessary every four time series. The data will be transferred to a computer located in the main control room of the ETW via a camera link interface using optical fibers leading to transfer times of a few minutes.

C. Planned Wall Interference Measurements

Standard measurements will be performed during testing including forces and moments, flow parameters and model pitch angle. Measurements of specific parameters such as pressure distribution on test section walls, wing deformation and model position in the test section are planned for the future CFD wall interference investigations.

A preliminary estimation of the ETW wall interference will be made based on comparison with NASA 11ft and NTF wind tunnel results (the blockage of CRM model is about 2 times less in NASA 11ft and 1.3 times less in NTF wind tunnels in comparison with ETW). The created database will allow to use different methods (classical and CFD) to investigate ETW slotted wall interference. The application of different methods should increase the accuracy and reliability of ETW test results and, consequently, the efficiency and safety of future aircraft performance predictions. One more outcome of this test campaign is to use experimental data as a complex test case for the validation and verification of different existing and upcoming CFD methods including the ones developed to solve the wall interference problem for transonic wind tunnels with slotted walls.

D. Test Matrix

A preliminary test program was defined (Tab. 2) that considers the scientific objectives of the wake and the wall interference studies and provides sufficient data for upcoming and future code validation purposes. Planned TR-PIV wake measurements are listed in Pos. 1-2 for the full configuration and in Pos. 8-9 for horizontal tail off case. Positions 6-7 are intended to compare experimental data with CFD results presented in the Drag Prediction Workshop 4 (DPW4)[32]. Comparison of experimental results in ETW and two NASA wind tunnels (NTF and 11ft) will be derived in positions 3-4 simultaneously with wall interference investigations. Four additional polars at $M_\infty = 0.697$; 0.703; 0.847; 0.853 (position 5) will serve for wall interference investigations to define the derivatives of model aerodynamic characteristics versus Mach number. It will be required in the future process of application of wall interference corrections – recalculation of corrected data to the required Mach number values.

V. Conclusion and Outlook

Within the ESWI^{RP} sub-project "Time-resolved wake measurements of separated wing flow and wall interference measurements" tests will be performed in the ETW facility on the NASA CRM model, representing a modern generic civil aircraft configuration. The objective on one side is to investigate the unsteady flow in the wake upstream of the empennage in stall conditions and on the other side to investigate wall interference effects.

For the unsteady wake studies conventional techniques of the, highly instrumented model but also advanced techniques will be used. In particular a cryo TR-PIV technique developed at DLR will be applied for unsteady flow field measurements. The measurements performed with this technique will constitute a unique database for unsteady wake development past civil aircraft configurations at both, low speed and high speed conditions. Numerical computations will also be performed with URANS and hybrid RANS / LES codes in order to support the preparation of the tests and to perform a numerical / experimental validation.

The experimental database will be public, as well as the geometry of the model, so that it could become a reference database for the analysis of such phenomena or for numerical codes validation. In addition, the tests will be an opportunity to operate the TR-PIV technique in the ETW facility, in order to improve the capabilities of this technique in an industrial environment as well as delivering to ETW new measurement capabilities.

On the topic of wall interference effects, these tests will deliver measurements that will be used for the development and the validation of new techniques for the determination of these effects, based on CFD computations. The validation of these techniques requires specific measurements that are not usually done. The project will be also an opportunity for ETW to improve their capabilities on this subject.

Acknowledgments

Financial support for the upcoming wind tunnel tests will be given by the European Commission in the 7th framework program. The authors would like to acknowledge the EC for funding this research and the partners of the consortium, the ESWI[RP] coordinators and the ETW team for the fruitful cooperation during the preparation phase of this project.

Table 2. Test matrix of planned ETW measurements.

Pos.	M_∞	*Re*, mln	Angle of attack	Transition	htp	Measurements			Remarks
						TR-PIV	Stan-dard	Wing deformatio	
1	0.85	30 5.8	2°, 2.5° … 5°	10%	0°	+	+	+	Wake measurements
2	0.25	17.2 5	8 alphas	10%	0°	+	+	+	Wake measurements
3	0.70 0.85	19.8 30	0.5°-5° (sweep +0.1°/s, -0.8°/s)	10%	0°	-	+	+	Wall interference and comparison with NTF
4	0.7 0.85	5	0.5°-5° (sweep +0.1°/s, -0.8°/s)	10%	0°	-	+	+	Wall interference and comparison with NTF and 11ft
5	0.697, 0.703, 0.847, 0.853	5	0.5°-5° (sweep +0.1°/s, -0.8°/s)	10%	0°	-	+	+	Wall interference
6	0.85	5	0.0°, 1.0°, 1.5°, 2.0°, 2.5°, 3.0°, 4.0°	10%	0°	-	+	+	DPW4
7	0.70, 0.78, 0.80, 0.83, 0.85, 0.86, 0.87		c_l = 0.400, 0.450, 0.500	10%	0°	-	+	+	DPW4
8	0.85	30 5.8	2°, 2.5° … 5°	10%	off	+	+	+	Wake measurements
9	0.25	17.2 5	8 alphas	10%	off	+	+	+	Wake measurements

References

[1]Ashill, P.R., Binion, T., Cooper, K.R., Crites, R., Everhart, J.L., Ewald, B.F., Hackett, J., Holst, H., Krynytzky, A.J., Malmuth, N.D., Mokry, M., Newman, P.A., Sickles, W.L., Steilne, F.W.J., Taylor, C.R., Taylor, N.J., Voss, R., Wedemeyer, E.H., "Wind Tunnel Wall Corrections", *AGARD Advisory Group for Aerospace Research and Development AGARD-AG-336*, 1998.

[2]Balakrishna, S., Acheson, M.J., "Analysis of NASA Common Research Model Dynamic Data," *AIAA 2011-112*, 2011.

[3]Bosniakov, S., "Experience in integrating CFD to the technology of testing models in wind tunnels," *Progress in Aerospace Sciences*, 1998, Vol. 34, pp. 391-422.

[4]Bosnyakov, S., Kursakov, I., Lysenkov, A., Matyash, S., Mikhailov, S., Vlasenko V., Quest, J., "Computational tools for supporting the testing of civil aircraft con-figurations in wind tunnels," *Progress in Aerospace Sciences*, 2008, v. 44, No 2, pp.67-120.

[5]Collercandy, R., Marques, B., Lory, J., Dbjay, S., Espiau, L., "Application of CFD for wall and sting effects," *HiReTT report HIRETTTNAFRCoWP2.2311002003*, Airbus France, October 2003.

[6]Deck, S., "Zonal Detached Eddy Simulation of the Flow around a High-Lift Configuration," *AIAA Journal*, Vol. 43, No 11, pp 2372-2384, Nov 2005.

[7]Deck, S., "Three-Element Airfoil," *DESider – A European Effort on Hybrid RANS-LES Modelling,* edited by Haase, W., Braza, M., Revell, A., pp. 127-139, Springer, Berlin, 2009.

[8]Durrani, N., Qin, N., "Behavior of Detached-Eddy Simulations for Mild Airfoil Trailing-Edge Separation," *Journal of Aircraft*, Vol. 48(1), pp. 193-202, 2011.

[9]Gansel, P.P., Illi, S.A, Lutz, T., Krämer, E., "Numerical Simulation of Low-Speed Stall and Analysis of Turbulent Wake Spectra," *Conference Modelling Fluid Flow '12, 15th International Conference on Fluid Flow Technologies*, Proc. Vol. I, pp. 199-206, Budapest, 4-7 Sep. 2012.

[10]Gansel, P.P., Dürr, P., Baumann, M., Lutz, T., Krämer, E., "Influence of Meshing on Flow Simulation in the Wing-Body Junction of Transport Aircraft," *18th STAB/DGLR Symposium*, Stuttgart, 6-7 Nov. 2012.

[11]Garbaruk, A., Shur, M., Strelets, M., Travin, A., "NACA0021 at 60° Incidence," *DESider – A European Effort on Hybrid RANS-LES Modelling* , edited by Haase, W., Braza, M., Revell, A., pp. 127-139, 2009.

[12]Havas, J., Rabadan, G.J., "Prediction of Horizontal Tail Plane Buffeting Loads," *IFASD-2009-128*, 2009.

[13]Hantrais-Gervois, J.L., Piat, J.F., "A Methodology to Derive Wind Tunnel Wall Corrections from RANS Simulations", *5th Symposium on integrating CFD and experiments in aerodynamics*, Tokyo, Japan, 2012.

[14]Illi, S.A., Fingskes, C., Lutz, T., Krämer, E., "Transonic Tail Buffet Simulations for the Common Research Model," *31th AIAA Applied Aerodynamics Conference*, San Diego, CA, June 24-27, 2013. (submitted for publication)

[15]Illi, S.A., Lutz, Th. and Krämer E., "Transonic Tail Buffet Simulations on the ATRA Research Aircraft," *Computational Flight Testing Results of the closing symposium of the German research initiative ComFliTe* edited by Kroll, N., Radespiel, R., van der Burg, J. and Sørensen, K., Braunschweig, Germany, Springer, 2013.

[16]Konrath, R., Otter, D., Geisler, R., Agocs, J., Mattner, H., Roosenboom, E.W.M., Fey, U., Quest, J., Kühn, C., "Adaptation of PIV for Application in Cryogenic Pressurized Wind Tunnel Facilities at High Reynolds Numbers" *Proc. of 15th International Symp. on Applications of Laser Techniques to Fluid Mechanics*, Lisbon, Portugal, Paper 1572, 05-08 July, 2010.

[17]Lehmkuhl, O., Baez, A., Rodríguez, I., Pérez-Segarra, C.D., "Direct Numerical Simulation and Large-Eddy Simulations of the Turbulent Flow around a NACA0012 Airfoil," *Proc. 7th International Conference on Comp. Heat and Mass Transfer*, Istanbul, Turkey, 2011.

[18]Lopez Mejia, O.D., Moser, R.D., Brzozowski, D.P., Glezer, A., "Effects of Trailing-Edge Synthetic Jet Actuation on an Airfoil," *AIAA Journal*, Vol. 49, No. 8, pp. 1763-1777, Aug. 2011.

[19]Lysack, P.D., Brungart, T.A., "Velocity Spectrum Model for Turbulence Ingestion Noise from Computational-Fluid-Dynamics Calculations," *AIAA Journal*, Vol. 41, No. 9, pp. 1827-1829, Sept. 2003.

[20]Melber-Wilkending, S., Heidebrecht, A., Wichmann, G., "A new approach in CFD supported wind tunnel testing," *25th International Congress of the Aeronautical sciences*, ICAS 2006, 3.4.2.

[21]Molton, P., Bur, R., Lepage, A., Brunet, V., Dandois, J., "Control of Buffet Phenomenon on a Transonic Swept Wing," *40th Fluid Dynamics Conference and Exhibit*, AIAA 2010-4595, 2010.

[22]Pope, S.B., *Turbulent Flows*, 8th printing, Cambridge University Press, UK, 2011.

[23]Probst, A., Radespiel, R., "A Comparison of Detached-Eddy Simulation and Reynolds-Stress Modelling Applied to the Flow over a Backward-Facing Step and an Airfoil at Stall," *Proc. 48th AIAA Aerospace Sciences Meeting including the New Horizons Forum and Aerospace Exposition*, Orlando, FL, AIAA-2010-920, 2010.

[24]Quest, J., Glazkov, S.A., Gorbushin, A.R., Ivanov, A.I., Semenov, A.V., Vlasenko, V.V., "Numerical and experimental Investigations of Slot Flow with Respect to Wind Tunnel Wall Interference Assessment," *24-th AIAA Aerodynamic Measurement technology and Ground Testing Conference*, Portland, Oregon, 28 June, 2004.

[25]Quest, J., Konrath, R., "Accepting a Challenge – The Development of PIV for Application in pressurized cryogenic Wind Tunnels," *41-th AIAA Fluid Dynamics Conference*, Honolulu, Hawai, June 27 -30, 2011.

[26]Schwamborn, D., Gerhold, T., Heinrich, R., "The DLR TAU-Code, Recent Applications in Research and Industry," *European Conference on Computational Fluid Dynamics ECCOMAS CFD 2006*, Wesseling, P., Oñate, E., Périaux, J. (Eds.), Delft, The Netherlands, 4-8 Sep. 2006.

[27]Seifert, A., Pack, L.G., "Oscillatory Excitation of Unsteady Compressible Flows over Airfoils at Flight Reynolds Numbers," *37th AIAA Aerospace Sciences Meeting and Exhibit*, AIAA 99-0925, Reno NV, 11-14 Jan 1999.

[28]Spalart, P.R., Allmaras, S.R., "A One-equation Turbulence Model for Aerodynamic Flows," *AIAA-92-0439*, 1992.

[29]Steimle, C.P., Karhoff, D.C., Schröder, W., "Unsteady Transonic Flow over a Transport-Type Swept Wing," *AIAA Journal Vol. 50*, No. 2, February 2012.

[30]Vassberg, J.C., DeHaan, M.A., Rivers, S.M., Wahls, R.A., "Development of a Common Research Model for Applied CFD Validation Studies," *AIAA 2008-6919*, 2008.

[31]Vaucheret, X., "Recent Calculation Progress on Wall Interferences in Industrial Wind Tunnels," *La Recherche Aerospatiale*, No 3, pp 45-47, 1988.

[32]Vassberg, J.C., Tinoco, E.N., Mani, M., Rider, B., Zickuhr, T., Levy, D.W., Broderson, O.P., Eisfeld, B., Crippa, S., Wahls, R.A., Morrison, J.H., Mavriplis, D.J., Murayama, M., "Summary of the Fourth AIAA CFD Drag Prediciton Workshop," *AIAA-2010-4547, 28th AIAA Applied Aerodynamics Conference*, Chicago, IL, 28 Jun - 1 Jul 2010.

[33]Weinman, K., "NACA0012 beyond Stall," *FLOMANIA – A European Initiative on Flow Physics Modelling*, edited by Haase, W., Aupoix, B., Burge, U., Schwammborn, D., pp. 233-246, 2006.

[34]Wokoeck, R., Grote, A., Krimmelbein, N., Ortmanns, J., Radespiel, R., Krumbein, A., "RANS Simulation and Experiments on the Stall Behaviour of a Tailplane Airfoil," *New Results in Numerical and Experimental Fluid Mechanics V*, edited by Rath, H.-J., Holze, C., Heinemann, H.-J., Henke, R., Hönlinger, H., Notes on Numerical Fluid Mechanics and Multidisciplinary Design, Vol. 92, pp. 208-216, 2006.